frontiers | Frontiers in Earth Science

TYPE Original Research
PUBLISHED 09 January 2023
DOI 10.3389/feart.2022.1031493

OPEN ACCESS

EDITED BY
Deyu Gong,
Research Institute of Petroleum Exploration and Development (RIPED), China

REVIEWED BY
Longyi Shao,
China University of Mining and Technology, China
Shuheng Tang,
China University of Geosciences, China

*CORRESPONDENCE
Yongshang Kang,
kangysh@sina.com

SPECIALTY SECTION
This article was submitted to Economic Geology,
a section of the journal
Frontiers in Earth Science

RECEIVED 30 August 2022
ACCEPTED 12 September 2022
PUBLISHED 09 January 2023

CITATION
Kang Y, Huangfu Y, Zhang B, He Z, Jiang S and Ma YZ (2023), Gas oversaturation in deep coals and its implications for coal bed methane development: A case study in Linxing Block, Ordos Basin, China.
Front. Earth Sci. 10:1031493.
doi: 10.3389/feart.2022.1031493

Gas oversaturation in deep coals and its implications for coal bed methane development: A case study in Linxing Block, Ordos Basin, China

Yongshang Kang[1,2]*, Yuhui Huangfu[3], Bing Zhang[4], Zhiping He[5], Shanyu Jiang[6] and Yuan Zee Ma[7]

[1]College of Geosciences, China University of Petroleum, Beijing, China, [2]State Key Laboratory of Petroleum Resources and Prospecting, China University of Petroleum, Beijing, China, [3]School of Earth and Space Sciences, Peking University, Beijing, China, [4]China United Coalbed Methane Corporation, Ltd, Beijing, China, [5]China Storage Energy, Beijing, China, [6]Consulting and Research Center of Ministry of Natural Resource, Beijing, China, [7]Schlumberger, Denver, CO, United States

Three coal bed methane (CBM) wells penetrating to coal seams 8+9# (Permian Taiyuan Formation), in deep coals (depth>1,500 m), show very differential production performance in Linxing Block, eastern margin of the Ordos Basin in China. The mechanism for the performance differentiation is analyzed through studies on coal permeability and gas saturation in deep coals, and specifically, the comparison of coal reservoir characteristics in the three wells. The mechanism for gas oversaturation is then discussed based on data from Linxing Block and spot but important exploration results relevant to deep coals in the Junggar Basin. This study demonstrates that: (1) Permeability values of coal seams 8+9# in deep coals are probably in the order of 10^{-2}mD from diverse sources including results of experimental permeability test simulating underground stress conditions. Studies on gas saturation distribution reveal that high gas rates (>3,000 m^3/d) can be achieved only from oversaturated coal reservoirs in Linxing Block. (2) Two types of oversaturation mechanism, including igneous intrusion-driven oversaturation and sorption capacity-driven oversaturation, exist in deep coals. The former is restricted to regions/blocks influenced by igneous intrusion, and characterized by secondary gas generation and supplementation to deep coals that have substantial similar Langmuir curves to that of shallow coals. The latter may play in deep coals that are not influenced by igneous intrusion, and is characterized by more free gas released from coals after adsorption saturation, due to reduced sorption capacity in deep coals; (3) Oversaturation may exist more frequently in deep coals (in comparison with shallow coals), due to mostly the sorption capacity-driven oversaturation mechanism, and the weaker tectonic deformation and uplifting experienced by deep coals in comparison with shallow coals, which favors gas preservation and oversaturation. (4) Generally, coal permeability in deep coals is low due to the increased effective stress, and exploring oversaturation areas should be a primary concern for CBM development. It appears that in most large, tectonically compressed coal basins, there is a critical depth beyond which

the oversaturation areas could occur, presenting opportunities and challlenges for CBM development.

KEYWORDS

CBM, gas oversaturation, Langmuir curve, production performance, permeability, deep coal

1 Introduction

Coals are mostly undersaturated with gas, because most coal basins have been variably uplifted from their maximum depth of burial (Bustin and Bustin, 2008; Seidle, 2011). Coal bed methane (CBM) production from undersaturated coals requires primary dewatering to induce desorption of adsorbed gas below the critical desorption pressure. Coal permeability and gas saturation are the two most vital parameters determining gas rate and CBM recovery (Moore, 2012).

Until now, the CBM development targets are mostly undersaturated shallow coals in China and also in other countries, although a large part of the world's coalbed methane resources is distributed in coal seams deeper than 1,500 m (Kuuskraa and Wyman, 1993; Johnson and Flores, 1998). A new round of CBM resource evaluation in China reported resources of about $30\times10^{12}m^3$, in the depth of 1,500–3,000 m (Li X. Z. et al., 2016). Notice that shallow coals and deep coals are divided with a burial depth of 1,500 m hereinafter.

Because of low permeability and low gas saturation, a large part of CBM blocks in shallow coals in China need long time primary dewatering (several months to more than 1 year), while produce at low gas rates then. Almost two-thirds of injection/falloff tested permeability values are inferior to 1 mD (Kang et al., 2017) and about half of tested samples are with saturation being lower than 60%, according to our recent statistical analysis. Low permeability and low gas saturation in shallow coals are due to complex tectonic evolution history and strong tectonic deformation and uplifting, specifically near the margins of compressional coal basins.

Although no much work has been done in deep CBM drilling and exploration due to the disadvantageous factors such as drilling cost and low permeability, several high gas rates from deep coals were reported. For example, tested gas rate in well Pinyon Ridge Federal A, in the Piceance basin, United States, was reported at 27,152 m^3/d (Kuuskraa and Wyman, 1993). In recent years, two CBM wells penetrating to deep coals in Linxing Block of the Ordos Basin in China have been found to produce gas directly, with almost zero water production and the gas rates are stable at a level of >3,000 m^3/d. However, one other nearby well penetrating to the same coal seams in deep coals has very low gas rate (<120 m^3/d). The production performance differentiation provides an opportunity to enhance the understandings on CBM in deep coals through discussion of coal permeability and gas saturation, and specifically, the comparison of coal reservoir characteristics in the three wells. Based on the understandings from Linxing Block, we will extend our discussion to a more general perspective on CBM in deep coals through integrating the spot but important exploration results relevant to deep coals in the Junggar Basin, where wells of similar performance were seen.

2 Backgrounds and CBM well production characteristics

2.1 Backgrounds

Linxing Block, with areal extent of 2,530 km^2, is located across the Yishan slope and the Jinxi flexural fold belt, in the eastern margin of the Ordos Basin (Figure 1A). The Zijinshan igneous rock outcrops are to the east of the Block (Figure 1B, Gu et al., 2016).

The coal seams 8+9$^{\#}$ and 4+5$^{\#}$, belonging to Permian Taiyuan Formation and Shanxi Formation respectively (Figure 2), are the main CBM targets. This study focuses on coal seams 8+9$^{\#}$ in Permian Taiyuan Formation, because three CBM wells in deep coals are producing from these coal seams. Figure 1B is the map showing the burial depth of coal seams 8+9$^{\#}$. They are buried from about 700 m to more than 2,000 m in the block. Shallow coals take a limited areal extent in the northeastern corner of block and deep coals (depth>1,500 m) are distributed in most part of the block. The coal seams 8+9$^{\#}$, deposited in peat-swamp facies of delta environments (Li Y. et al., 2016; Li et al., 2017b), are laterally continuous with the thickness range of 3.6–15.4 m, and an average of 7.9 m.

Most wells in Linxing Block are commingled production wells from coal seams 8+9$^{\#}$ and/or coal seams 4+5$^{\#}$, and overlying tight sandstones. The production performance of the commingled production wells will not be analyzed in this paper, due to the complexity from gas/water bearing tight sandstones. It is impossible to extract any valuable information about gas saturation states of coal seams of 8+9$^{\#}$ from these wells' production performance. Only three vertical wells penetrating to deep coals, including wells LX-29, LXX-23–2 and LXX-24 (see Figure 1B for well locations), are producing from coal seams 8+9$^{\#}$. The production performance of the three vertical wells will be compared in the following.

Laboratory tested porosity, maceral composition and proximate analysis on coal samples taken from coal seams 8+9$^{\#}$, are found in Supplementary Appendix S1. These data

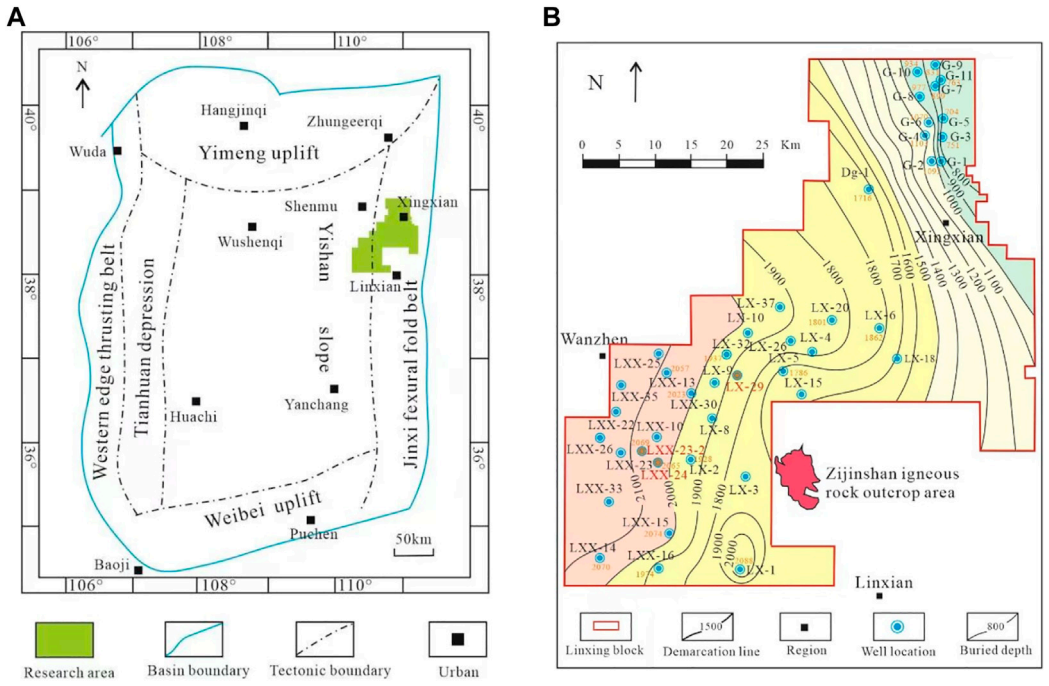

FIGURE 1
Location map **(A)**, burial depth of coal seams 8+9# **(B)**in Linxing Block.

will be used to analyze the influencing factors of coal sorption capacity.

In-situ gas content, methane compositional proportion (%), laboratory tested R_o (%), Langmuir parameters (air-dry basis) tested at formation temperature, on coal samples taken from coal seams 8+9#, are found in Supplementary Appendix S2. These data will be used to compare the Langmuir curves between shallow coals and deep coals, and to estimate gas saturation.

2.2 CBM well production characteristics

As mentioned above, three wells including LX-29, LXX-23–2 and LXX-24 (see Figure 1B for well locations), are producing from coal seams 8+9#. All the three wells were completed by hydrofracturing techniques with similar parameters. However, the wells have very different performance characteristics and can be lumped into two types (Figure 3).

1) Well LX-29 behaves as a normal CBM well that needs to pump out water before gas production. The coal seams 8+9# in well LX-29 are buried from 1,879.7 m to 1,907.7 m. Production began on 24 October 2017. The well was drained for up to 3 months before the onset of gas production (Figure 3A). Both the water production and gas production are very low, implying the permeability (no available data) is too low to produce any fluids in a significant amount.

2) Two wells, including LXX23-2 and LXX-24, have obtained high gas production without primary dewatering. These wells produced gas after hydraulic fracturing without installing any pump (Figures 3B,C).

Coal seams 8+9# in well LXX-23–2 are buried from 2,059.5m to 2,069.0 m. In April 2017, the coal seams 8+9# were hydro-fractured with slickwater. Gas production began after 3-day's flowing. The daily gas production from July 2017 to March 2018 was stable at 3,100–3,500 m^3 (Figure 3B), and the daily water production was less than 0.5 m^3 (water production curve is not shown in Figure 3B).

Coal seams 8+9# in well LXX-24, are buried from 2,013.4 m to 2,019.5 m. In November 2017, Coal seams 8+9# were hydro-fractured with slickwater and after only 2-day's flowing, gas began to produce. By September 2018, the daily gas production was stable at 3,200–3,600 m^3 (Figure 3C), and the daily water production was less than 1 m^3 (water production curve is not shown in Figure 3C).

The mechanism for the performance differentiation will be studied through discussion of permeability and saturation in deep coals (depth>1,500 m), and specifically, the comparison of coal reservoir characteristics in the three wells.

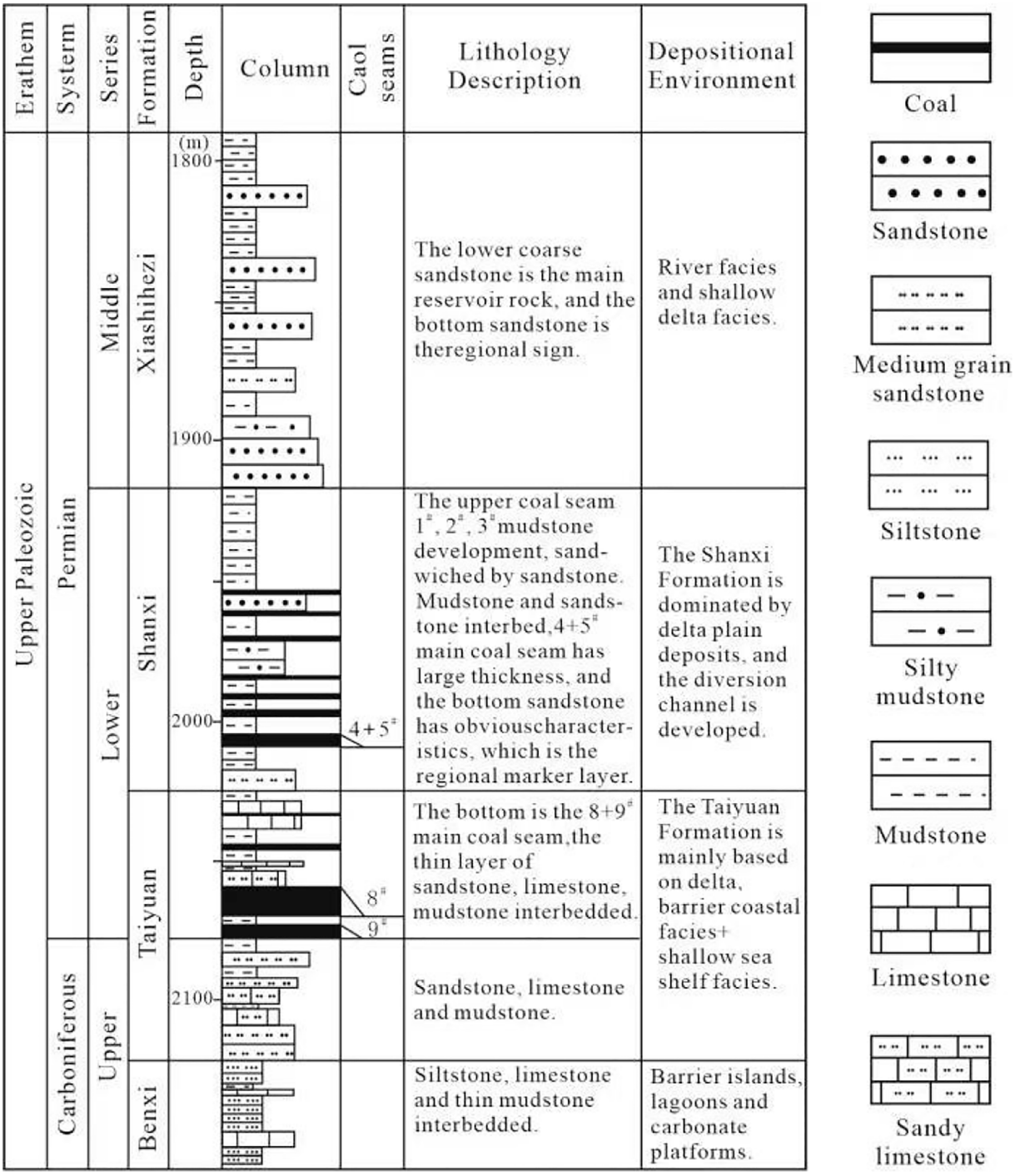

FIGURE 2
Stratigraphic column of coal measures (Li et al., 2017b; Shao et al., 2018) in Linxing Block.

3 Permeability in deep coals

Porosity data of coal samples taken from coal seams 8+9# are available in deep coals (see Supplementary Appendix S1). The location of wells used to collect samples can be found in Figure 1B. Figure 4A shows coal porosity variation with depth in deep coals. No obvious trend in porosity can be observed from 1,712.7 m to 2,088.1 m. The porosity values

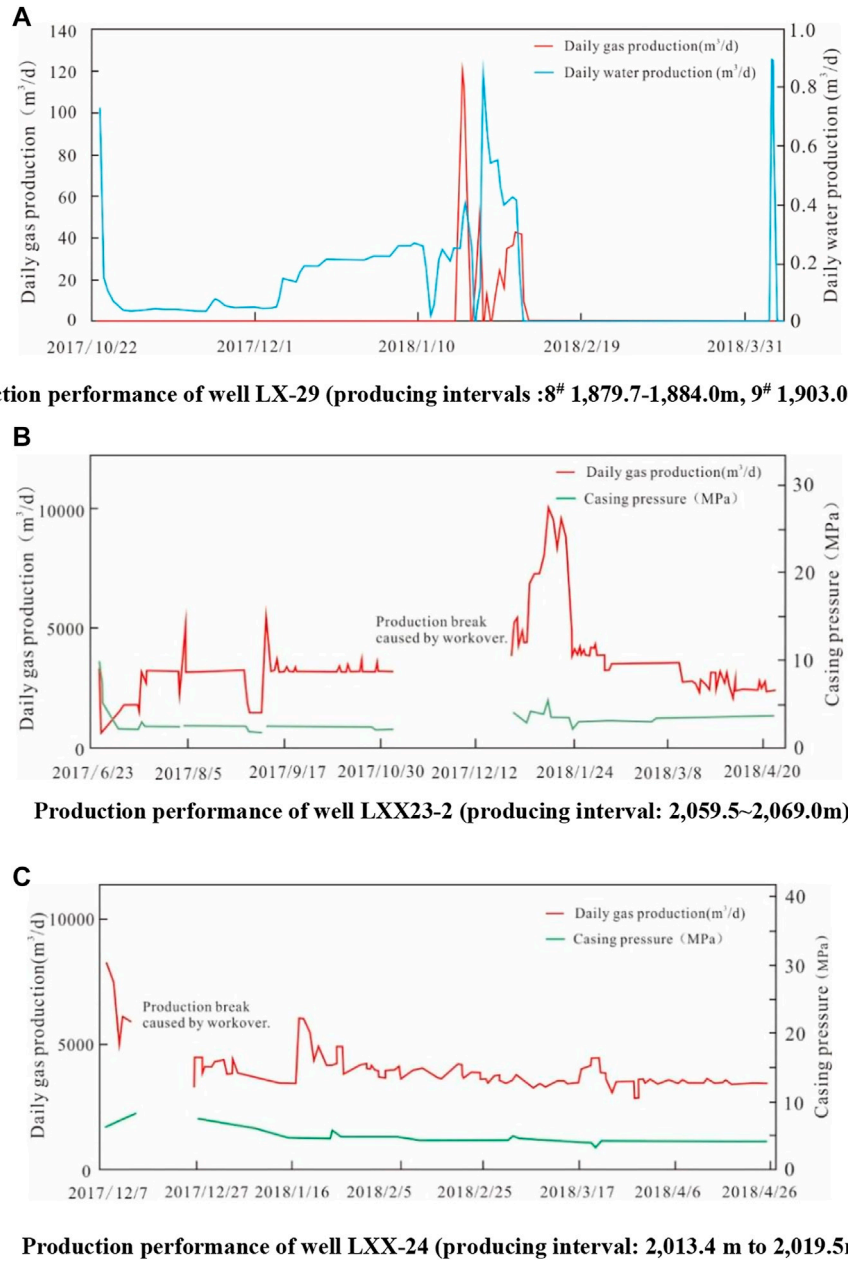

FIGURE 3
Production performance of CBM wells in Linxing CBM Block. **(A)** Production performance of well LX-29 (producing intervals :8# 1,879.7-1,884.0 m, 9# 1,903.0-1,907.7 m). **(B)** Production performance of well LXX23-2 (producing interval: 2,059.5~2,069.0 m). **(C)** Production performance of well LXX-24 (producing interval: 2,013.4 m to 2,019.5 m). (All the three wells are producing from coal seams 8+9# in Taiyuan Formation. Wells LXX23-2 and LXX24 had no water production. These wells were put on production after hydraulic fracturing without water pumping out).

range from 3.14 to 6.79%, with an average of 4.70% (Figure 4A).

The only one injection/falloff test of coal seams 8+9# in the block was done in well LXX-22 (see Figure 1B for well location). The interpretation indicates that the permeability of coal seams 8+9# is of 0.8×10^{-2}mD for the tested interval of 2,007.0–2,020.0 m.

Coal permeability is strongly stress-dependent. In laboratory studies, measured permeability of coal samples under different stress, in general, declined exponentially with increasing effective stress (Pomeroy and Robinson, 1966; Somerton et al., 1975; McKee et al., 1988a; Sparks et al., 1995; Bustin, 1997; Meng and Li, 2013; Bottomley et al., 2017). Due to the rising effective

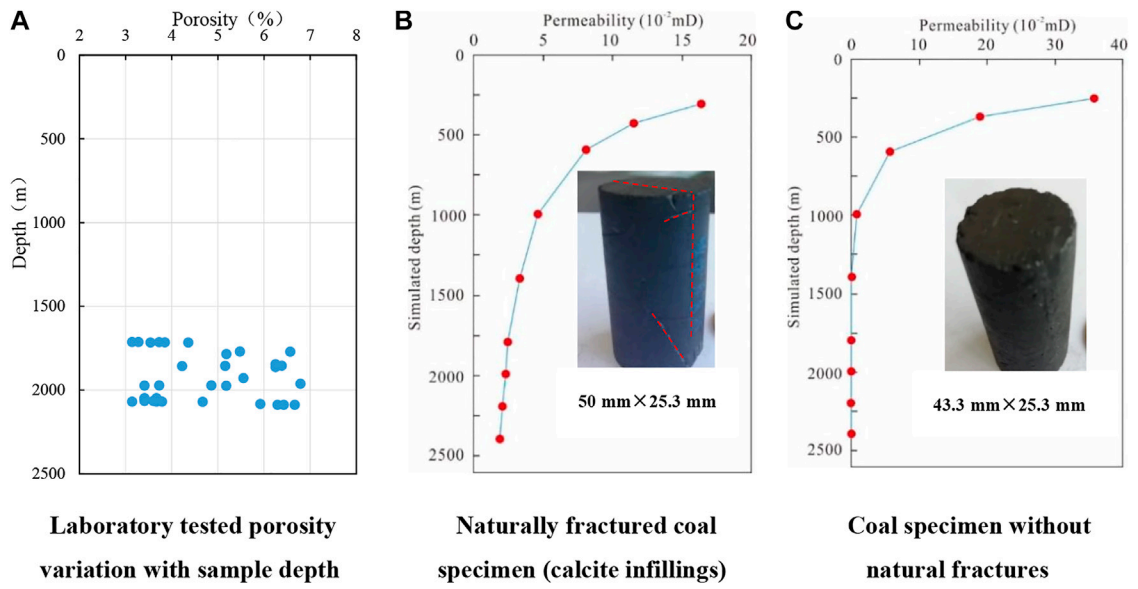

FIGURE 4
Laboratory tested porosity **(A)**, and results of experimental permeability test simulating underground stress conditions with simulated depth **(B)** and **(C)**. (Coal samples were taking from mines in or near Linxing Block)

stress with increasing depth, an exponential relation between coal permeability and depth was previously identified in the Piceance, San Juan, and Black Warrior basins, United States (McKee et al., 1988a; 1988b), in major coalbed methane (CBM) basins of Australia (Enever et al., 1994; Enever and Hennig, 1997; ScottMazumder and Gibson, 2013; Mukherjee and CopleyEsterle, 2017), as well as in some CBM blocks in Qinshui and Ordos basins, central China (Meng et al., 2011; Tao et al., 2014; Liu et al., 2016).

For simulating experimentally coal permeability values with increasing depth, eight blocky coal samples were taken from mines in or near Linxing Block, in eastern margin of the Ordos Basin, and prepared to cylindrical specimens. Among the eight specimens, only one is naturally fractured (fractures are infilled with calcite) and the measured permeability values in deep coals (simulated depth >1,500 m) are in the order of 10^{-2}mD (Figure 4B). No natural fractures or cleats were observed in all the other seven specimens, and the measured permeability values, in deep coals (simulated depth >1,500 m), are approaching to zero. Figure 4C presents the experimental results of one of these seven specimens. Comparing Figures 4B, C, difference in simulated permeability volume in depth is remarkable.

In the experimental permeability test simulating underground stress conditions, permeability values were measured using helium gas when axial pressure and confining pressure were loaded simultaneously on the tested specimen, with a lateral pressure ratio of 0.7. This ratio corresponds to the average lateral stress ratio in deep coals in eastern margin of the Ordos basin (Li et al., 2018; Wen et al., 2019). More concretely, the axial pressure and confining (lateral) pressure are determined by:

$$\sigma_v = \rho g h = 2.3{*}9.8h = 22.54h \quad (1)$$

$$\sigma_h = 0.7\sigma_v = 15.778h \quad (2)$$

where, $\sigma_v$and$\sigma_h$are axial pressure and confining (lateral) pressure, MPa, respectively; h is the simulated depth, 10^3 m.

For a simulated depth, for example, of 2000 m, in Figures 4B, C, an axial pressure of 45.08 MPa and a confining (lateral) pressure of 31.56 MPa are adapted for the tri-axial test.

Notice that our laboratory tested permeability values of the naturally fractured specimen (Figure 4B) are in agreement, from (simulated) depth 1,524 m (5,000 ft) to 1,829 m (6,000 ft), with the theoretically estimated values through Kozeney-Carman equation in Mckee et al. (1988a, their Figure 7), although the permeability values are very different in shallow (simulated) depths (<1,000 m) in the two comparative cases.

The experimental results shown in Figures 4B,C indicate that the permeability in deep coals is not only influenced by *in-situ* stress, but also by coal body structure. Coal-body structure, classified as normal, cataclastic, granular and mylonitic types in China's CBM applications (GB/T 30050, 2013), is an indicator of tectonic deformation degree that coals have been experienced. From normal to mylonitic types, the deformation gets stronger. Compared with normal type, cataclastic type contributes to permeability, while granular and mylonitic types destruct permeability (Kang et al., 2017).

TABLE 1 Statistical comparison of coal-body structure between shallow and deep coals in Linxing Block.

Shallow coals (depth<1,100 m)			Deep coals (depth>1,600 m)		
Structure type	Frequency (%)	Sum (%)	Structure type	Frequency (%)	Sum (%)
Normal	8.64	30.86	Normal	20.69	96.55
Cataclastic	22.22		Cataclastic	75.86	
Granular	32.10	69.14	Granular	1.15	3.45
Mylonitic	37.04		Mylonitic	2.30	

Notice: Totally 168 coal-body structure description records of cores in Linxing Block were collected. Among the 168 records, 81 records were assigned to shallow coals (<1100 m) and 87 records were assigned to deep coals (>1600 m).

TABLE 2 Logging Interpretation results for coal seams 8+9# and average daily gas production in wells LXX 23–2 and LXX-24.

Well	Top depth (m)	Bottom depth (m)	Thickness (m)	Porosity (%)	Permeability (10^{-2}mD)	Average daily gas production (m^3/d)
TB-23–2	2,059.5	2,069.0	9.5	4.3	1	3,181
TB-24	2,013.40	2,019.50	6.1	3.9	6	3,942

Due to the fact that cataclastic type is the predominant coal-body structure type (75.86%) in deep coals in Linxing Block (Table 1), it is believed that the permeability values in deep coals are probably in the order of 10^{-2}mD according to Figure 4B.

Logging interpretations show that the permeability values of coal seams 8+9# in wells LXX23-2 and LXX-24 are of 1×10^{-2}mD and 6×10^{-2} mD respectively (Table 2), which are in agreement with the experimental results from naturally fractured specimen (Figure 4B).

Permeability data from diverse sources presented above, including results from experimental permeability test simulating underground stress conditions, indicate that the permeability values of coal seams 8+9# in LXX23-2 and LXX-24 are probably in the order of 10^{-2}mD. The permeability value of coal seams 8+9# in well LX-29 is inferred to be in the same order or even a little higher, considering that the burial depth of coal seams 8+9# in this well is of 1,879.7–1,907.7 m, while the burial depths of coal seams 8+9# in wells LXX23-2 and LXX-24 are respectively of 2,059.5–2,069 m and 2,013.4–2,019.5 m. However, the production performance of wells LXX23-2 and LXX-24 is very different from that of well LX-29 (Figure 3). Besides permeability, gas saturation is another vital parameter to be considered.

Lacking test data of *in-situ* gas content and Langmuir parameters in the three wells, gas saturation values of coal seams 8+9# in these wells cannot be estimated directly. The gas saturation states of coal seams 8+9# in the three wells will be inferred from gas saturation distribution maps drawn from data in other wells in the block.

4 Gas saturation in deep coals

4.1 Comparison of Langmuir curves between shallow coals and deep coals

In-situ gas sorption capacity can be described by Langmuir equation (Langmuir, 1918):

$$V_t = V_L \times P/(P_L + P) \quad (3)$$

where, P is the formation pressure, MPa; V_L (m^3/t) and P_L (MPa) are the Langmuir volume and Langmuir pressure respectively, tested at formation temperature (°C); V_L (m^3/t) represents the maximum sorption capacity at formation temperature (°C) when pressure increases to infinite, which is called hereinafter sorption capacity.

Previous studies have demonstrated that the sorption capacity (V_L) decreases with increasing temperature, while P_L increases with increasing temperature (Ottiger et al., 2010). At a preset temperature, the sorption capacity increases with increasing vitrinite (Lamberson and Bustin, 1993; Clarkson and Bustin, 1996). Moisture is a competing factor to gas adsorption, which reduces the sorption capacity (Joubert et al., 1973; Yalçin and Durucan, 1991; Krooss et al., 2002). Mineral matter or ash is a diluent to the sorption capacity (Lamberson and Bustin, 1993; Crosdale et al., 1998). The sorption capacity increases with increasing rank (Levy et al., 1997; Bustin and Clarkson, 1998; Laxminarayana and Crosdale, 1999).

We initially focus on the differences, regarding the influencing factors of sorption capacity, between deep coals and shallow coals. Figure 5A demonstrates that deep coals

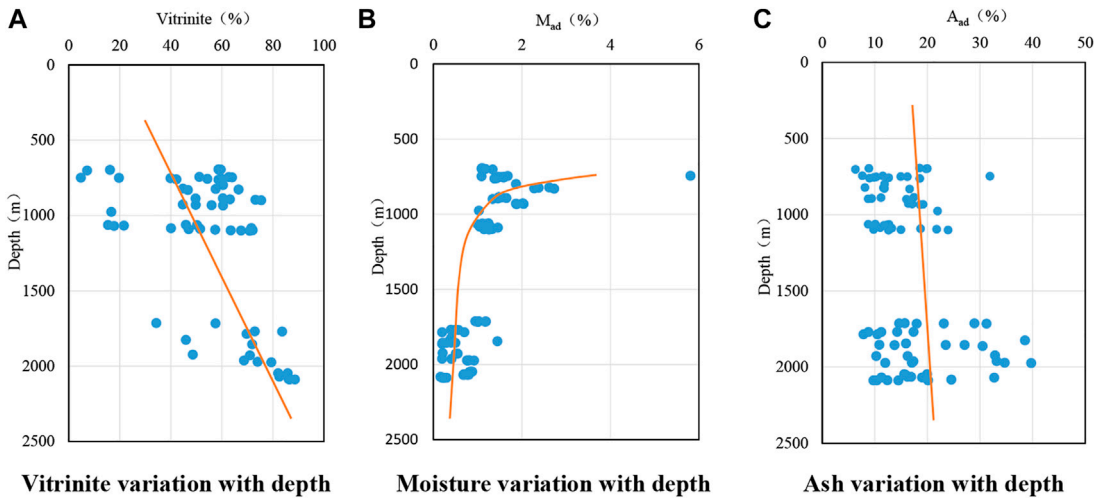

FIGURE 5
Diagram showing vitrinite **(A)**, moisture **(B)** and ash variations **(C)** with depth.

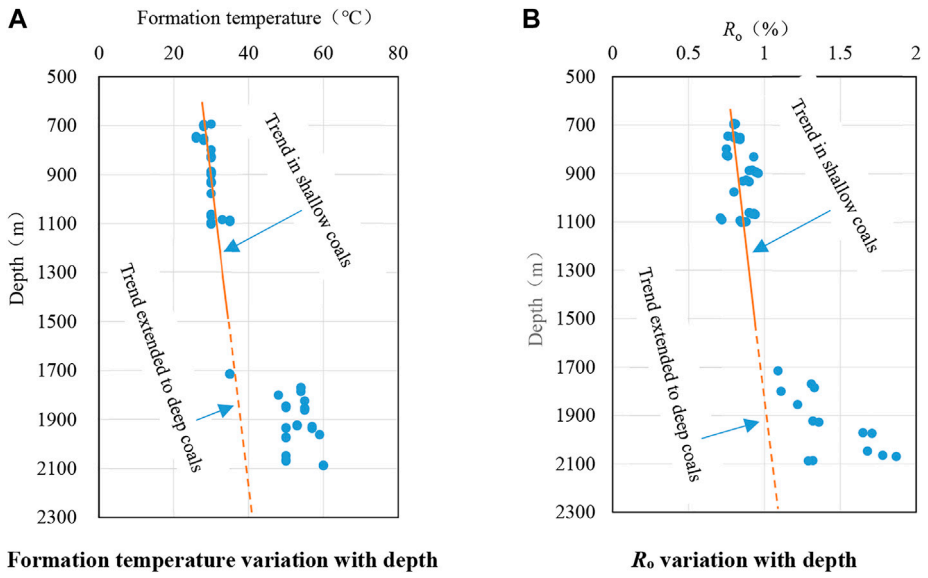

FIGURE 6
Diagram showing variations of formation temperature **(A)** and R_o **(B)**, with depth in Linxing Block.

have higher vitrinite than shallow coals. The difference may be caused by coal deposition environments and coal rank variation (Li et al., 2017a). Figure 5B demonstrates that moisture decreases with increasing depth. Deep coals generally have lower moisture than shallow coals. Figure 5C demonstrates that ash is almost random from shallow coals to deep coals.

Practically, formation temperature and coal rank both related to depth (Figure 6), can be considered as the two most important parameters determining Langmuir curves. In Langmuir curve comparison between shallow coals and deep coals, other influencing factors of sorption capacity are less important, since these factors either are related more or less to coal rank (such as vitrinite and moisture), or almost can be considered as random (such as ash) with increasing depth (Figure 5).

As can be seen, from Figure 6, that either the formation temperature (Figure 6A) or the coal rank (Figure 6B) in deep coals, deviate abnormally from the trend lines determined by shallow coals. The high-value anomalies in formation

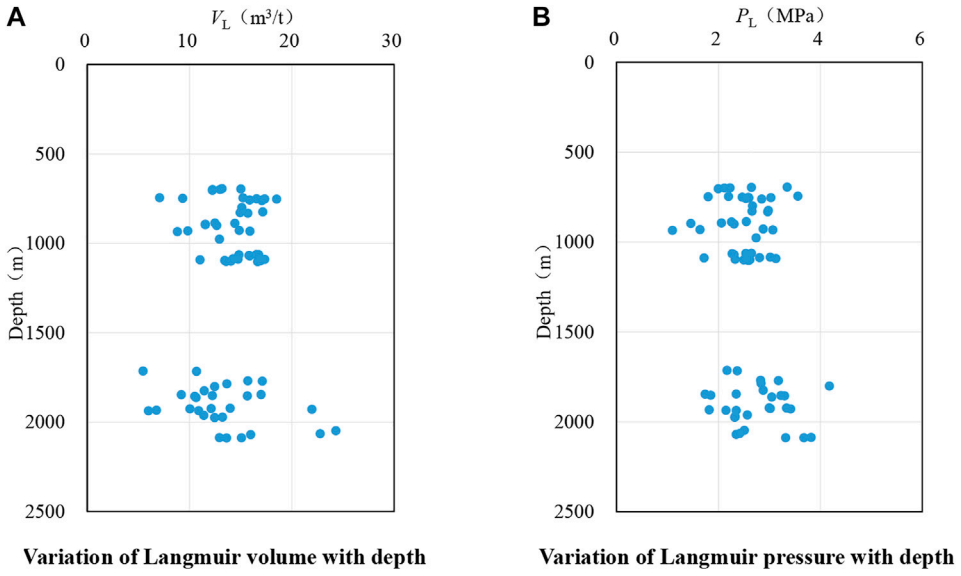

FIGURE 7
Diagram showing variations of Langmuir volume (sorption capacity) **(A)**, Langmuir pressure **(B)** with depth in Linxing Block.

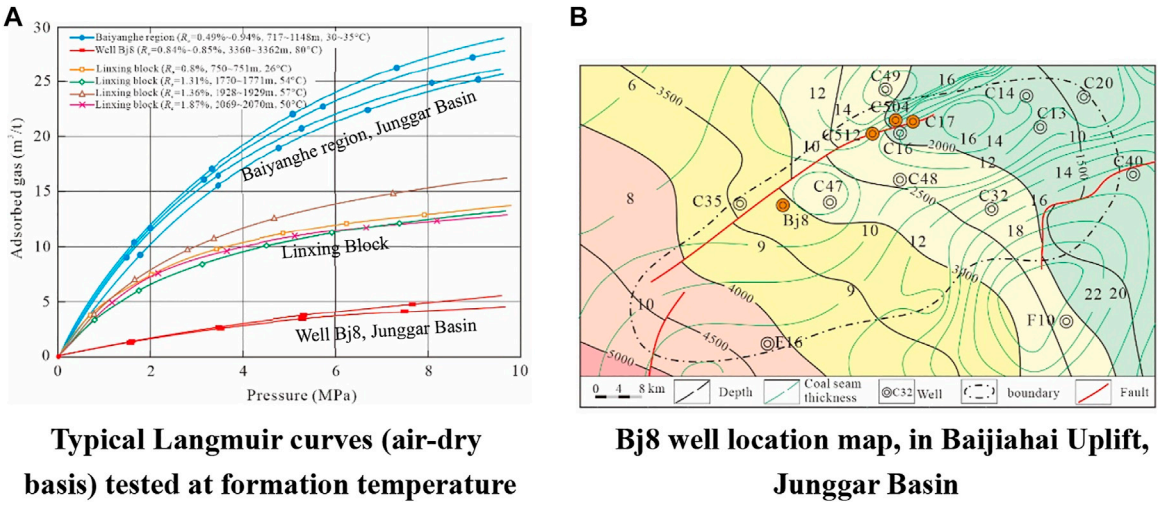

FIGURE 8
Typical Langmuir curves (air-dry basis) **(A)**, tested at formation temperature. In different depths in Linxing Block and in the Junggar Basin, and Bj8 well location **(B)**.

temperature and coal rank in deep coals are due to the Zijinshan igneous intrusion (Fu et al., 2016). Figure 6 indicates also that the shallow coals have not been influenced by the igneous intrusion. The sorption capacity relies on several factors such as vitrinite content, vitrinite reflection and temperature. The sorption capacity increases with vitrinite content and vitrinite reflection that increase with increasing depth (Figure 5A, Figure 6B), and decreases with temperature that increases with increasing depth (Figure 6A). Two opposite, increasing and decreasing factors of the sorption capacity make it almost stable with increasing depth (Figure 7A; Figure 8A).

The combined effect of abnormally increased temperature (reduction of sorption capacity), and increased rank and increased vitrinite content (increase of sorption capacity) in

deep coals, results in almost undifferentiated sorption capacity (Langmuir volume) and Langmuir pressure between deep coals and shallow coals, as shown in Figure 7.

Figure 8A shows that the Langmuir curves in deep coals are substantially similar to that in shallow coals in Linxing Block. Figure 8B shows the well location of Bj8.

However, according to our observations from several cases which are absent of influence of igneous intrusion, coal rank does not necessarily increase obviously with increasing depth, although the formation temperature does increase, following the geothermal gradient, with increasing depth. In these cases, the Langmuir curves in deep coals may be very different from that of shallow coals. As an example, Langmuir curves in shallow coals (Jurassic Badaowan Formation coals in Baiyanghe region) and in deep coals (Jurassic Xishanyao Formation coals in well Bj8, Figure 8B for well location) are very distinguishable in the Junggar Basin, western China (Figure 8A). In contrast to the case in Linxing Block, the sorption capacity (V_L) of deep coals, in the Junggar Basin, is highly reduced in comparison with that of shallow coals. The average sorption capacity (V_L) of four Jurassic Badaowan Formation coal samples, in shallow coals, is of about 26m^3/t (air-dry basis). The four samples ranked as sub-bituminous to high bituminous (R_o: 0.49–0.94%), were taken from wells in Baiyanghe region in depth interval of 717.0–1,148.0 m with formation temperature of 30°C–35°C. Remarkably, the average sorption capacity of two Jurassic Xishanyao Formation coal samples, in deep coals, is reduced to only of 6m^3/t (air-dry basis). The two samples ranked as high volatile bituminous (R_o: 0.84%–0.86%), were taken from well Bj8 in depth interval of 3,360.4–3,363.2 m with formation temperature of 80°C.

The implication of Langmuir curve differentiation between shallow coals and deep coals in the Junggar Basin will be discussed later.

4.2 Gas saturation distribution

Gas saturation is defined as:

$$S_g = 100\% \times V_r / V_t \quad (4)$$

where, V_r is the *in-situ* gas content, m^3/t, measured usually through canister desorption method; V_t is the *in-situ* gas sorption capacity (calculated at formation temperature and pressure), m^3/t. The *in-situ* gas sorption capacity (V_t), can be estimated by Langmuir Equation 3.

In reality, the *in-situ* gas content includes methane and other gases (such as carbon dioxide and nitrogen), whereas the Langmuir parameters are usually determined by using pure methane. Direct use of Equation 4 may induce over-estimation of gas saturation (Seidle, 2011). For precluding the multi-component impact on gas saturation estimation, the following equation is used for methane saturation estimation:

$$S_m = 100\% \times V_{rm} / V_{tm} \quad (5)$$

where, V_{rm} is the *in-situ* methane content (m^3/t) that can be estimated from *in-situ* gas content multiplied by the methane compositional proportion (%); V_{tm} is the *in-situ* methane sorption capacity (m^3/t) (calculated at formation temperature and pressure).

Notice that the methane saturation in Equation 5 is only a precise estimation for gas saturation. The term "gas saturation" is still used hereinafter as a general expression, except where the methane saturation is specifically referred.

By using Equation 5, the methane saturation was estimated for coal samples with *in-situ* gas content and Langmuir test data. For comparison, methane saturation estimation results and related parameters, in shallow coals (694.2–1,102.8 m depth interval, 43 coal samples) and in deep coals (1,716.2–2,088.3 m depth interval, 28 coal samples) in Linxing Block, are set forth in Supplementary Appendix S2. All the coal samples in Supplementary Appendix S2 were taken from coal seams 8+9#. The location of wells used to collect samples can be found in Figure 1B. The formation pressure (column 10 in Supplementary Appendix S2) for each coal sample is estimated as the product of the sample burial depth and the average pressure gradient of 0.9 MPa/100 in the block (Li et al., 2018). The formation pressure so estimated may bear some bias. This bias does not, however, influence the reliability of saturation estimation, since the formation pressure in deep coals (depth>1,500 m) is generally higher than 10 MPa beyond which the *in-situ* sorption capacity is almost stable with increasing formation pressure (Figure 8).

As can be seen, from column 12 in Supplementary Appendix S2, that shallow coals (694.2–1,102.8 m depth interval) are gas undersaturated with methane saturation from 11.72% to 64.48%, while the methane saturation in deep coals (1,716.2–2,088.3 m depth interval) is from 32.10% to 197.10%. By using the estimated methane saturation in column 12 in Supplementary Appendix S2, three alternative maps are drawn to show methane saturation distribution in coal seams 8+9# in Linxing Block (Figures 9A–C).

Since there are often two or more sample saturation values and the sample number is limited in individual wells, uncertainty exists in saturation assignment to the wells. Figures 9A–C are drawn by using the maximum sample saturation value, the average sample saturation value and the minimum sample saturation value in individual wells, respectively. Correspondingly, Figures 9A–C represent the optimistic, probable and pessimistic scenarios of methane saturation distribution respectively, based on available data. Figure 9D is the map of gas content that confirms the probable scenario (Figure 9B), considering that the Langmuir curves are

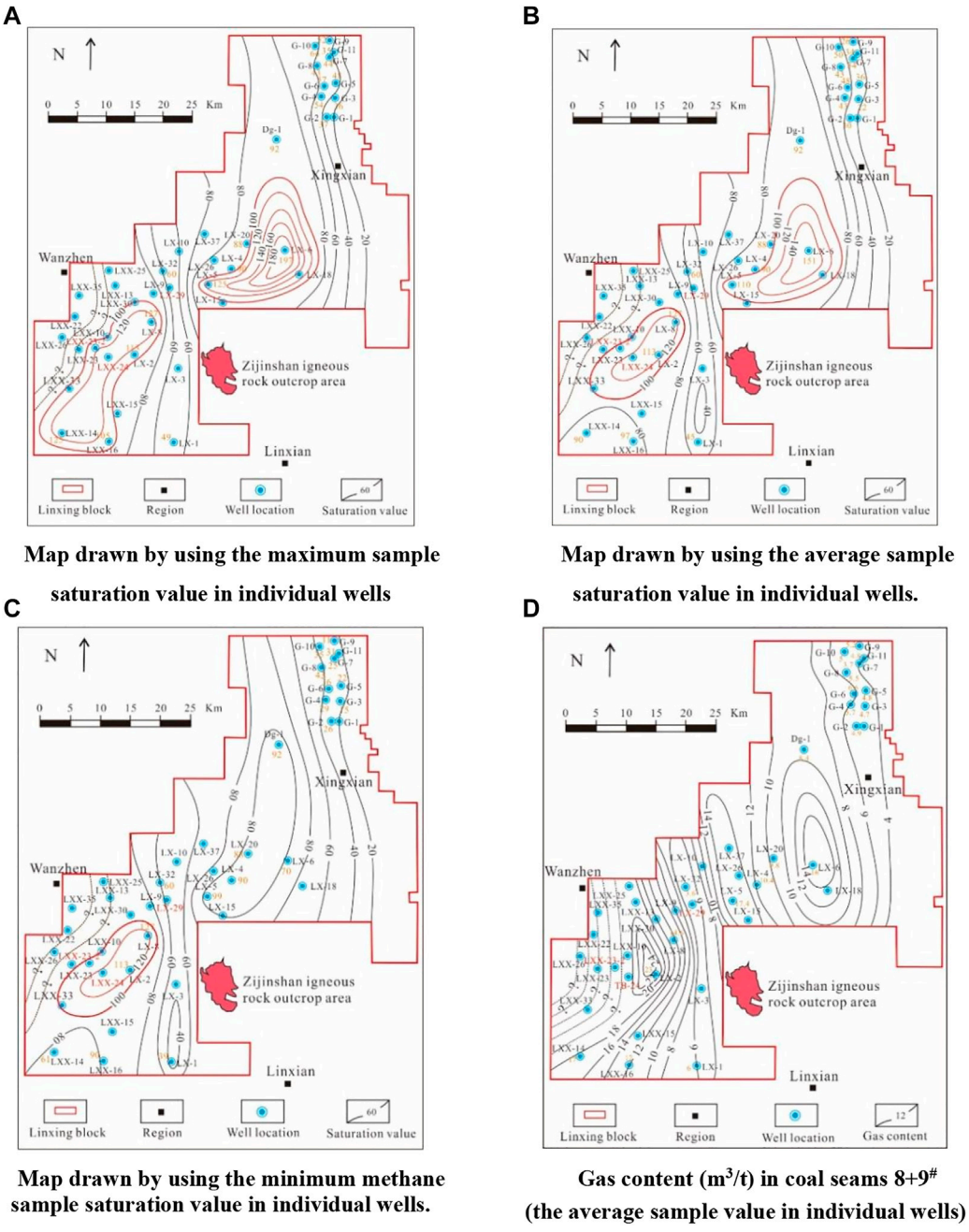

FIGURE 9
Alternative maps showing methane saturation in coal seams 8+9 # **(A–C)** and gas content **(D)** in Linxing Block (oversaturation zones are marked by red contour). (Note: A faulted zone along the line of well LX-10 and well LX-1, can be seen clearly in Li et al., 2018, their Figure 1, which corresponds to a low methane saturation zone in **(A–C)**.

substantially similar in different depths in Linxing Block (Figure 8).

Figures 9A–C demonstrate that oversaturation is not pervasive in deep coals. Rather, two oversaturation zones likely exist (Figure 9B), one in the center of the block and the other in the west of the block. Notice that the drilling cores from coal seams 8+9# in Well LXX-33 were observed with very intense and fast gas flow out when immerged in water, indicating that the coal seams 8+9# in this well bear *in-situ* free gas and the coal reservoirs are oversaturated. This well is contoured within the west oversaturation zone in Figures 9A–C, although no saturation value is estimated due to lack of coal sample test data in this well.

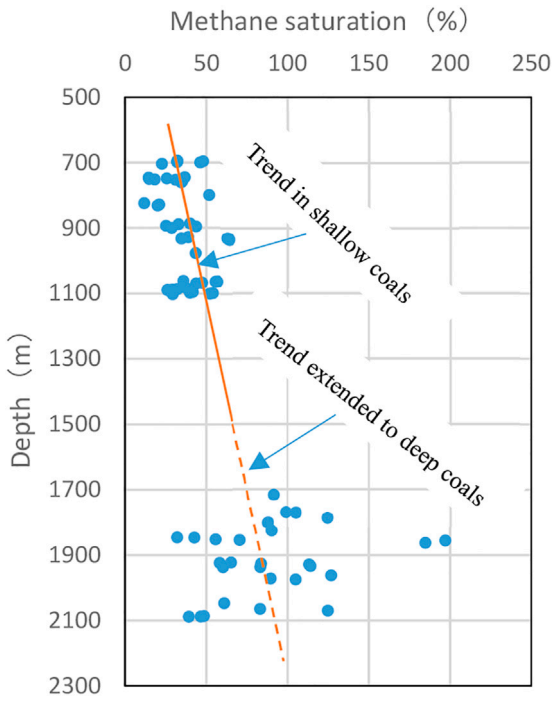

FIGURE 10
Diagram of methane saturation with depth, coal seams 8+9, Linxing Block.

Importantly, the two wells LXX23-2 and LXX-24 that produce gas directly without primary dewatering and have stable and high gas rates (>3,000m^3/d), can be both with great certainty delineated within the west oversaturation zone on any map in Figures 9A–C. While the well LX-29 that produce very low gas (<120 m^3/d) after about 3 months of dewatering, can be evidently contoured outside the oversaturation zones on any map in Figures 9A–C. Moreover, the diagram of gas (methane) saturation with depth shows clearly that there exist oversaturated and undersaturated coal reservoirs in deep coals (Figure 10). The mechanism for oversaturation will be discussed later.

5 Discussion

5.1 Mechanism for production performance differentiation

Well LX-29, producing gas from coal seams 8+9$^{\#}$ with a net coal thickness of 9m, is outside the methane oversaturation zones (Figures 9A–C). In undersaturated coals, the fluid phases are assumed to include irreducible water, free water, adsorbed gas, and possibly minor solution gas. Primary dewatering must be performed to reduce reservoir pressure to below the critical desorption pressure for gas desorption and production. Because of low permeability (in the order of 10^{-2}mD) and permeability sensitivity to increasing effective stress during dewatering, the depression cone cannot be extended far from the borehole, resulting in very low gas rates (<120 m^3/d) in this well.

It is very exciting that the two wells LXX23-2 and LXX-24 have reached high and stable gas rates (>3,000m^3/d), although the permeability values of coal seams 8+9$^{\#}$ are as low as in the order of 10^{-2}mD. Notice that the thickness of producing coal seams 8+9$^{\#}$, in wells LXX23-2 and LXX-24, is of 9.5 and 6.1 m respectively.

As shown above, coal seams 8+9$^{\#}$ in wells LXX23-2 and LXX-24 are almost certain to be gas oversaturated. In oversaturated coals, the fluid phases are assumed to include irreducible water, minor free water, adsorbed gas, minor solution gas and *in-situ* free gas. *In-situ* free gas is ready to migrate to the borehole, and the forerunner flow out of the *in-situ* free gas draws reservoir pressure down, resulting in the desorption of adsorbed gas (in saturated state) immediately. Water production is limited by high relative permeability of gas phase and low water content in deep coals (see Figure 5B). Gas is much easier to migrate than water, resulting in high gas production and very low or negligible water production.

The above interpretation is a simplified description of the real-world complex two-phase (water and gas) or even three-phase (water, gas and coal fines) flow in oversaturated coals. Works need to be done for better understanding the flowing phases at the beginning of production with different *in-situ* free gas saturation and in different coals. Different coals may have very differentiable relative permeability curves that are difficultly tested in laboratory with comparable results, although many scholars have done a lot of works for understanding coal relative permeability with the selected coals in their study cases (e.g., Conway et al., 1995; Meaney and Paterson, 1996; Shedid and Rahman, 2009). However, a conclusion can be drawn as that gas saturation states (undersaturation or oversaturation) are the most vital factor determining production performance of CBM wells in deep coals. High gas rates (>3,000m^3/d) can be achieved only from oversaturation zones in deep coals with permeability values being as low as in the order of 10^{-2}mD, in Linxing Block.

The term “oversaturated coals” used in this paper represents the coals which are gas oversaturated and bearing *in-situ* free gas, and can also bear minor free water in macroscopic pores (>50nm, according to IUPAC, 1982) and fractures. The term “dry coals” is frequently used by many scholars for representing no water CBM wells in shallow coals (Bastian et al., 2005; Hoch, 2005; Seidle, 2011). Shallow dry coals in Horseshoe Canyon, Alberta may also bear *in-situ* free gas (Bustin and Bustin, 2011). There may exist different mechanism for the occurrence of *in-situ* free gas between shallow coals and deep coals. The shallow dry coals in Horseshoe Canyon, Alberta, are characterized with extremely

low formation pressure (Bastian et al., 2005), this is evidently not the case in deep coals in Linxing Block.

5.2 Mechanism for oversaturation in deep coals

5.2.1 Igneous intrusion-driven oversaturation mechanism

Linxing Block is near the Zijinshan igneous rock outcrop area. The Zijinshan igneous intrusion took place mainly during late Jurassic to early Cretaceous (Tang et al., 2000; Chen et al., 2012), which had caused secondary gas generation (Tang et al., 2000). Gas supplied by the secondary gas generation might have increased the gas saturation to oversaturated state within the influence halo of the igneous intrusion in deep coals.

After crystallization and solidification of the intruded magma, two stages of uplift-cooling, including the early slow stage from 120 Ma (early Cretaceous) to 30 Ma (early Oligocene), and the later fast stage initiated at about 30 Ma, have happened (Chen et al., 2012). During the uplift-cooling stages, many small faults outgoing from the intrusion massif and a faulted zone along the western boundary of the intrusion massif, almost in N-S direction, have developed (Wu et al., 2018). This faulted zone, along the line of well LX-10 and well LX-1 in Figure 9, can be seen clearly in Li et al. (2018, their Figure 1). As conduits of gas escape and migration, the small outgoing faults and the faulted zone might have decreased gas saturation to an undersaturation state around the intrusion massif and along the faulted zone (for example, in Well LX-1). The previously-formed pervasive oversaturation area, within the influence halo of the igneous intrusion, might have been either separated into two oversaturation zones (Figures 9A,B) or reduced to the present-day west oversaturation zone (Figure 9C).

Figure 10 shows that gas saturation in shallow coals has a general increasing trend (solid line) with depth. Remind that the shallow coals have not been influenced by the igneous intrusion. With the increasing trend in shallow coals being extended to deep coals, it can be perceived that the saturation in deep coals consists of high oversaturation and deep undersaturation superimposed on an increasing saturation trend (dashed line) related to depth. The trend line is persistent from shallow coals, as if the igneous intrusion had not happened. This implies that beyond a certain depth, saying about 2200m, the coals could be yet oversaturated while the influence of igneous intrusion is absent. In fact, a persistent increasing saturation trend with depth was reported as well in Yanchuannan Block, eastern margin of the Ordos Basin, by Hou et al. (2016).

In Figure 10, the points characterized by high oversaturation to the extreme right of the trend line (dashed line) can be related to gas supplementation by the secondary gas generation mentioned above. While the points characterized by deep undersaturation to the extreme left of the trend line can be related to gas escape induced by the small outgoing faults and the faulted zone mentioned above.

The oversaturation mechanism in Linxing Block can be termed as igneous intrusion-driven oversaturation, which is characterized by secondary gas generation and supplementation to deep coals that have substantial similar Langmuir curves to that of shallow coals (Figure 8). Secondary gas generation necessary to supplement deep coals, superimposed on the persistent increasing saturation trend with depth, results in oversaturation (Figure 10). However, faults are destructive to oversaturation and may excite deep undersaturation in deep coals.

5.2.2 Sorption capacity-driven oversaturation mechanism

Importantly, the igneous intrusion-driven oversaturation mechanism is not the only mechanism in deep coals. Oversaturation may occur in deep coals due to the reduced sorption capacity shown above in the Junggar Basin (Figure 8A). Most coals have generated greater amounts of methane than they have the capacity to retain at some point in the high volatile bituminous rank range (if not earlier) (Levine, 1993). Due to the reduced sorption capacity in deep coals, more free gas may be released from coals after adsorption saturation, and kept completely or partially in coals as *in-situ* free gas compressed by increased pressure in deep coals, and coal reservoirs are thus oversaturated. For example, in well BJ8 in the Junggar Basin, the gas saturation in Jurassic coals (3,360.4–3,363.2 m) was estimated to be of 213.78–220.08% (Sun et al., 2017). Moreover, two nearby wells named Cai504 and Cai17, have been found to produce gas, without primary dewatering, from Jurassic coal seams buried in depth interval of 2,567.0–2,828.8 m. The stable gas rates from the two wells are of 2,300 m^3/d and 8,870 m^3/d, respectively (Zhi and Xue, 2013).

In the Junggar Basin, the oversaturation mechanism in deep coals can be termed as sorption capacity-driven oversaturation mechanism, which is characterized by more free gas released from coals after adsorption saturation, due to reduced sorption capacity in deep coals (Figure 8A). The reduction of sorption capacity is caused by the formation temperature-coal rank configuration in the Junggar Basin, which is characterized by a normal increase of formation temperature accompanied by a subtle coal rank increase with depth. Remind that in the Junggar Basin, from depth interval of 717–1148 m (in Baiyanghe region) to depth interval of 3,360.4–3,363.2 m (well Bj8), the formation temperature increases from 30–35°C–80°C, whereas coal rank (R_o) varies from 0.49–0.94% to 0.84–0.86%. The average sorption capacity (V_L) is dramatically reduced from about 26 m^3/t (air-dry basis) to about 6m^3/t (air-dry basis).

5.3 Perspective on CBM in deep coals

Oversaturation may exist more frequently in deep coals in comparison with in shallow coals, mostly due to the sorption

capacity-driven oversaturation mechanism. The formation temperature-coal rank configuration in the Junggar Basin, is not unique according to our preliminary observations elsewhere. This phenomenon has not been well documented and interpreted. Further works should be done in coal burial and thermal history studies. Notice that in the Aroma Basin, United States, the Hartshorne coal rank is interpreted as related to the maximum burial depth and accompanied heat flows in geological history and does not follow the present-day burial depths (Cardott, 2013).

Moreover, the weaker tectonic deformation and uplifting experienced by deep coals in comparison with shallow coals, favors gas preservation and oversaturation in deep coals. As can be seen from Table 1, more than half of coals are of granular and mylonitic types (69.14%) indicating a stronger tectonic deformation and related stronger uplifting in shallow coals. However, the coal-body structure is mostly of normal and cataclastic types (96%) in deep coals indicating a weaker tectonic deformation and related weaker uplifting. Although Table 1 is based on the coal-body structure data from Linxing Block, this observation may be generalized at least to most of the compressional basins. In fact, compressional tectonic force exerts on the margin of basins and attenuates to the center of the basins (Wang, 1992).

Our experimental permeability test simulating underground stress conditions demonstrates that the permeability values in deep coals are low (in the order of 10^{-2}mD or even lower). Kuuskraa and Wyman (1993) proposed a model predicting much higher permeability values in deep coals, specifically in low and moderate stress regions, but no supporting data from either experimental results or field were presented by them. In low permeability deep coals, exploring oversaturation areas should be a primary concern for CBM development in deep coals. It appears that in most large, tectonically compressed coal basins, there is a critical depth beyond which the oversaturation areas could occur. This critical depth is constrained by geothermal gradient, "coal rank gradient", formation pressure gradient and possibly along with other less important factors. The combined geothermal gradient and "coal rank gradient" may be the most predominant factors.

The oversaturation in deep coals provides opportunities and challenges for CBM development. Because of limited CBM drilling activities in deep coals, the understandings about the CBM in deep coals are limited. Many geological, geophysical and engineering issues related to CBM development in deep coals are to be studied while more data will be available through enhanced drilling in the future. These issues include, but not limited to: 1) The critical burial depth at which the oversaturation areas occur in different basins; 2) The conditions for basins in which coal rank has subtle increase from shallow coals to deep coals; 3) Geological conditions of oversaturation areas below the critical depth; 4) Geophysical technologies for identification and evaluation of oversaturated reservoirs in deep coals; 5) *In-situ* stress and permeability in deep coals; 6) Optimization of fracturing design and technologies; 7) Production regime control and technologies from deep coals.

6 Conclusion

From our study on the CBM field in Linxing Block, along with spot but important exploration results relevant to deep coals in the Junggar Basin, the following conclusions can be drawn:

1) Permeability data from diverse sources, including results of experimental permeability test simulating underground stress conditions, indicate that the permeability values of coal seams 8+9# in deep coals are probably in the order of 10^{-2}mD in Linxing Block.
2) Studies on gas saturation distribution reveal that high gas rates (>3,000 m^3/d) can be achieved only from oversaturated reservoirs with such low permeability in the order of 10^{-2}mD in Linxing Block.
3) Two types of oversaturation mechanism, including igneous intrusion-driven oversaturation and sorption capacity-driven oversaturation, exist in deep coals. The former is restricted to regions/blocks influenced by igneous intrusion such as in Linxing Block, and characterized by secondary gas generation and supplementation to deep coals that have substantial similar Langmuir curves to that of shallow coals. The latter may play in deep coals that are not influenced by igneous intrusion such as in the Junggar Basin and is characterized by more free gas released from coals after adsorption saturation, due to reduced sorption capacity in deep coals.
4) The reduction of sorption capacity in deep coals is caused by the formation temperature-coal rank configuration in the Junggar Basin, which is characterized by a normal increase of formation temperature accompanied by a subtle coal rank increase with depth. This configuration in the Junggar Basin is not unique. Oversaturation may exist more frequently in deep coals in comparison with in shallow coals, due to mostly the sorption capacity-driven oversaturation mechanism.
5) The weaker tectonic deformation and uplifting experienced by deep coals in comparison with shallow coals, is evidenced by statistical comparison of coal-body structure between shallow and deep coals in Linxing Block. This observation may be generalized at least to most of the compressional basins. The weaker tectonic deformation and uplifting favors gas preservation and oversaturation in deep coals.
6) Generally, the permeability is low in deep coals, due to the increased effective stress, and exploring oversaturation areas should be a primary concern for CBM development. It appears that in most large, tectonically compressed coal basins, there is a critical depth beyond which the oversaturation areas could occur, presenting opportunities and challenges for CBM development. Because of limited CBM drilling activities in deep coals, the understandings of

the CBM are limited. Many geological, geophysical and engineering issues related to CBM development in deep coals are to be studied while more data will be available through enhanced drilling in the future.

Data availability statement

The original contributions presented in the study are included in the article/Supplementary Material, further inquiries can be directed to the corresponding author.

Author contributions

YK offered a main idea to this research and accomplish this paper mainly. YH, BZ and ZH take part in some research and write this paper. SJ and YM help collect some data and put some useful advice for this paper.

Funding

This work was financially sponsored by National Science and Technology Major Projects of China (2016ZX05041-001 and 2016ZX05044-005). The authors would like to thank all the group members for providing valuable advice to accomplish this paper.

Conflict of interest

Author BZ was employed by the company China United Coalbed Methane Corporation, Ltd. Author YM was employed by the company Schlumberger.

The remaining authors declare that the research was conducted in the absence of any commercial or financial relationships that could be construed as a potential conflict of interest.

Publisher's note

Supplementary material

The Supplementary Material for this article can be found online at: https://www.frontiersin.org/articles/10.3389/feart.2022.1031493/full#supplementary-material.

References

Bastian, P. A., Wirth, O. F. R., Wang, L., and Voneiff, G. W. (2005). "Assessment and development of dry Horseshoe Canyon CBM play in Canada," in 2005 Annual Technical Conference and Exhibition, Dallas, Texas, U.S.A., October 2005, 9–12.

Bottomley, W., Furniss, J. P., Raza, S. S., Ge, L., and Rudolph, V. (2017). "Characterizing the dependence of coal permeability to methane adsorption, pore pressure and stress; laboratory testing of Walloon coals from the Surat basin," in SPE/ATMI Asia Pacific Oil & Gas conference and exhibition, Jakarta, Indonesia, 17-19 October, 2017.

Bustin, A. M. M., and Bustin, R. M. (2008). Coal reservoir saturation: Impact of temperature and pressure. *Am. Assoc. Pet. Geol. Bull.* 92 (1), 77–86. doi:10.1306/08270706133

Bustin, A. M. M., Bustin, R. M., and Russel-Houston, J. (2011). Horseshoe Canyon and belly river coal measures, south central Alberta: Part 2 - modeling reservoir properties and producible gas. *Bull. Can. Petroleum Geol.* 59 (3), 235–260. doi:10.2113/gscpgbull.59.3.235

Bustin, R. M., and Clarkson, C. R. (1998). Geological controls on coalbed methane reservoir capacity and gas content. *Int. J. Coal Geol.* 38, 3–26. doi:10.1016/s0166-5162(98)00030-5

Bustin, R. M. (1997). Importance of fabric and composition on the stress sensitivity of permeability in some coals, northern sydney basin, Australia: Relevance to coalbed methane exploitation. *AAPG Bull.* 81 (11), 1894–1908.

Cardott, B. J. (2013). Hartshorne coal rank applied to Arkoma Basin coalbed methane activity, Oklahoma, USA. *Int. J. Coal Geol.* 108, 35–46. doi:10.1016/j.coal.2011.07.002

Chen, G., Ding, C., Xu, L. M., Zhang, R. H., Hu, Y. X., Yang, F., et al. (2012). Analysis on the thermal history and uplift process of Zijinshan intrusive complex in the eastern Ordos basin. *Chin. J. Geophys.* 55 (11), 3731–3741.

Clarkson, C. R., and Bustin, R. M. (1996). Variation in micropore capacity and size distribution with composition in bituminous coal of the Western Canadian Sedimentary Basin: Implications for coalbed methane potential. *Fuel* 75, 1483–1498. doi:10.1016/0016-2361(96)00142-1

Conway, M. W., Mavor, M. J., Saulsberry, J., Barree, R. B., and Schraufnagel, R. A. (1995). "Multi-phase study flow properties for coalbed methane wells: A laboratory and field study," in 1995 Joint Rocky Mountain Regional Meeting and Low-Permeablity Reservoirs Symposium, Denver.

Crosdale, P. J., Beamish, B. B., and Valix, M. (1998). Coalbed methane sorption related to coal composition. *Int. J. Coal Geol.* 35, 147–158. doi:10.1016/s0166-5162(97)00015-3

Enever, J. R., and Hennig, A. (1997). "The relationship between permeability and effective stress for Australian coals and its implication with respect to coalbed methane exploration and reservoir modeling," in International Coalbed Methane Symposium Proceedings, the University of Alabama, Tuscaloosa, USA, 12~17 May.

Enever, J. R., Pattison, C. I., McWatters, R. H., and Clark, I. H. (1994). "The relationship between *in-situ* stress and reservoir permeability as a component in developing an exploration strategy for coalbed methane in Australia," in SPE/ISRM Rock Mechanics in Petroleum Engineering Conference, Delft, The Netherlands, 29~31 August.

Fu, N., Yang, S. C., He, Q., Xu, W., and Lin, Q. (2016). High-efficiency reservoir formation conditions of tight sandstone gas in Linxing-Shenfu Blocks on the east margin of Ordos Basin. *Acta Pet. Sin.* 37 (S1), 111–120.

GB/T 30050 (2013). *Classification of coal-body structure*. Beijing: Chinese Standards Press, 1–25.

Gu, J. Y., Zhang, B., and Guo, M. Q. (2016). Deep coalbed methane enrichment rules and its exploration and development prospect in Linxing Block. *J. China Coal Soc.* 41 (01), 72–79.

Hoch, O. (2005). "The dry coal anomaly-the Horseshoe Canyon formation of Alberta, Canada," in 2005 Annual Technical Conference and Exhibition, Dallas, Texas, U.S.A., 9-12 October 2005.

Hou, S. H., Wang, X. M., Wang, X. J., Yuan, Y., and Zhuang, X. (2016). Geological controls on gas saturation in the yanchuannan coalbed methane field, southeastern Ordos basin, China. *Mar. Petroleum Geol.* 78, 254–270. doi:10.1016/j.marpetgeo.2016.09.029

IUPAC (1982). Manual of symbols and terminology. Appendix 2, Part 1, Colloid and surface chemistry. *Pure Appl. Chem.* 52, 2201.

Johnson, R. C., and Flores, R. M. (1998). Developmental geology of coalbed methane from shallow to deep in Rocky Mountain basins and in Cook Inlet–Matanuska basin, Alaska, U.S.A. and Canada. *Int. J. Coal Geol.* 35, 241–282. doi:10.1016/s0166-5162(97)00016-5

Joubert, J. I., Grein, C. T., and Bienstock, D. (1973). Sorption of methane in moist coal. *Fuel* 52, 181–185. doi:10.1016/0016-2361(73)90076-8

Kang, Y. S., Sun, L. Z., Zhang, B., Gu, J. Y., Ye, J. P., Jiang, S. Y., et al. (2017). The controlling factors of coal bed reservoirs permeability and CBM development strategy in China. *Geol. Rev. (in Chinese with English abstract)* 63 (5), 1401–1418.

Krooss, B. M., van Bergen, F., Gensterblum, Y., Siemons, N., Pagnier, H. J. M., and David, P. (2002). High-pressure methane and carbon dioxide adsorption on dry and moisture-equilibrated Pennsylvanian coals. *International Journal of Coal Geology* 51, 69–92. doi:10.1016/s0166-5162(02)00078-2

Kuuskraa, V. A., and Wyman, R. E. (1993). "Deep coal seams: An overlooked source for long-term natural gas supplie," in The SPE Gas Technology Symposium, Calgary, Alberta, Canada, 26-30 June.

Lamberson, M. N., and Bustin, R. M. (1993). Coalbed methane characteristics of Gates Formation coals, northeastern British Columbia: effect of maceral composition. *American Association of Petroleum Geologists Bulletin* 77, 2062–2076.

Langmuir, I. (1918). The adsorption of gases on plane surfaces of glass, mica and platinum. *J. Am. Chem. Soc.* 40, 1361–1403. doi:10.1021/ja02242a004

Laxminarayana, C., and Crosdale, P. J. (1999). Role of coal type and rank on methane sorption characteristics of Bowen Basin Australia coals. *International Journal of Coal Geology* 40, 309–325. doi:10.1016/s0166-5162(99)00005-1

Levine, J. R. (1993). "Coalification: The evolution of coal as source rock and reservoir rock for oil and gas," in *Hydrocarbons from coal, AAPG studies in Geology*. Editors B. E. Law and D. D. Rice, 39–77.

Levy, J. H., Day, S. J., and Killingley, J. S. (1997). Methane capacities of Bowen Basin coals related to coal properties. *Fuel* 76 (9), 813–819. doi:10.1016/s0016-2361(97)00078-1

Li, S., Tang, D., Pan, Z., Xu, H., Tao, S., Liu, Y., et al. (2018). Geological conditions of deep coalbed methane in the eastern margin of the Ordos Basin, China: Implications for coalbed methane development. *J. Nat. Gas Sci. Eng.* 53, 394–402. doi:10.1016/j.jngse.2018.03.016

Li, X. Z., Wang, Y. H., Jiang, Z. C., Chen, Z. L., Wang, L. Z., and Wu, Q. (2016a). Progress and study on exploration and production for deep coalbed methane [J]. *Journal of China Coal Society* 41 (01), 24–31.

Li, Y., Cao, D., Wu, P., Niu, X., and Zhang, Y. (2017a). Variation in maceral composition and gas content with vitrinite reflectance in bituminous coal of the eastern Ordos basin, China. *Journal of Petroleum Science and Engineering* 149, 114–125. doi:10.1016/j.petrol.2016.10.018

Li, Y., Tang, D., Wu, P., Niu, X., Wang, K., Qiao, P., et al. (2016b). Continuous unconventional natural gas accumulations of Carboniferous-Permian coal-bearing strata in the Linxing area, northeastern Ordos basin, China. *Journal of Natural Gas Science and Engineering* 36, 314–327. doi:10.1016/j.jngse.2016.10.037

Li, Y., Tang, D. Z., and Niu, X. L. (2017b). Sedimentary features of C-P coal bearing strata controlled by variation of accommodation spaces in east margin of Ordos Basin. *Journal of China Coal Society* 42 (7), 1828–1838.

Liu, H. H., Sang, S. X., Xue, J. H., Wang, G., Xu, H., Ren, B., et al. (2016). Characteristics of an *in-situ* stress field and its control on coal fractures and coal permeability in the Gucheng Block, southern Qinshui basin, China. *Journal of Natural Gas Science and Engineering* 36, 1130–1139. doi:10.1016/j.jngse.2016.03.024

McKee, C. R., Bumb, A. C., and Koenig, A. (1988b). "Stress dependent permeability and porosity of coal and other geological formation," in 1984 SPE/DOC/GRI Unconventional Gas Recovery Symposium, Pittsburgh, 13~15, May.

McKee, C. R., Bumb, A. C., and Koenig, A. (1988a). Stress dependent permeability and porosity of Coal[J]. *Rocky Mountain Association of Geologist* 3 (1), 143–153.

Meaney, K., and Paterson, L. (1996). "Relative permeability in coal," in 1996 SPE Asia Pacific Oil&Gas Conference, Adelaide.

Meng, Z. P., and Li, G. Q. (2013). Experimental research on the permeability of high-rank coal under a varying stress and its influencing factors. *Engineering Geology* 162, 108–117. doi:10.1016/j.enggeo.2013.04.013

Meng, Z. P., Zhang, J. C., and Wang, R. (2011). *In-situ* stress, pore pressure and stress-dependent permeability in the southern Qinshui basin. *Int. J. Rock Mech. Min. Sci. (1997).* 48, 122–131. doi:10.1016/j.ijrmms.2010.10.003

Moore, T. A. (2012). Coalbed methane: A review. *International Journal of Coal Geology* 101, 36–81. doi:10.1016/j.coal.2012.05.011

Mukherjee, S., CopleyEsterle, J. J., et al. (2017). "*In-situ* stress and fracture controls on permeability distribution within Walloon Subgroup, Surat basin," in SPE/ATMI Asia Pacific Oil & Gas conference and exhibition, Jakarta, Indonesia, 17-19 October, 2017.

Ottiger, S., Pini, R., Storti, G., Mazzotti, M., Bencini, R., Quattrocchi, F., et al. (2010). Adsorption of pure carbon dioxide and methane on dry coal from the sulcis coal province (SW Sardinia, Italy). *Environ. Prog.* 25 (4), 355–364. doi:10.1002/ep.10169

Pomeroy, C. D., and Robinson, D. J. (1966). The effect of applied stress on the permeability of a middle rank coal to water. *International Journal of Rock Mechanism and Mining Science* 4, 329–343.

ScottMazumder, M. S., Gibson, M., et al. (2013). "Application of open-hole diagnostic fracture injection test results to regional stress interpretation in Bowen basin coals," in SPE Unconventional Resource Conference and Exhibition-Asia Pacific, Brisbane, Australia, 11-13 November 2013.

Seidle, J. (2011). *Fundamentals of coalbed methane reservoir engineering.*

Shao, L. Y., Zheng, M. Q., Hou, H. H., Dong, D. X., and Wang, H. S. (2018). Characteristics sequence–palaeogeography and coal accumulation of Permo–Carboniferous coal measures in Shanxi Province. *Coal Science and Technology* 46 (2), 1–8.

Shedid, S. A., and Rahman, K. (2009). "Experimental Investigations of Stress-Dependent Petrophysical Properties and Reservoir Characterization of Coalbed Methane (CBM)," in Asia Pacific Oil and Gas Conference & Exhibition, Jakarta.

Somerton, W. H., Söylemezoğlu, I. M., and Dudley, R. C. (1975). Effect of stress on permeability of coal. *International Journal of Rock Mechanics and Mining Sciences & Geomechanics Abstracts* 12, 129–145. doi:10.1016/0148-9062(75)91244-9

Sparks, D. P., Mclendon, T. H., Saulsberry, J. L., and Lambert, S. W. (1995). "The effects of stress on coalbed reservoir performance, Black Warrior basin, U.S.A. SPE30734," in SPE Annual Technical Conference and Exhibition, Dallas, TX, October 22–25.

Sun, B., Yang, M. F., Yang, Q., Tian, W. G., Sun, Q. P., and Xu, Y. G. (2017). Analysis on occurrence state of deep coalbed methane in Junggar basin. *J. China Coal Soc.* 42 (A1), 195–202.

Tang, D. Z., Wang, J. L., Zang, J. F., and Huang, W. H. (2000). Secondary hydrocarbon generation of coal and accumulation of coalbed methane in the east margin of the Ordos Basin. *Experimental Petroleum Geology* 22 (2), 140–145.

Tao, S., Tang, D., Xu, H., Gao, L., and Fang, Y. (2014). Factors controlling high-yield coalbed methane vertical wells in the Fanzhuang Block, southern Qinshui basin. *International Journal of Coal Geology* 134 (135), 38–45. doi:10.1016/j.coal.2014.10.002

Wang, P. (1992). A geomechanical technique—types and distribution of geostress under various tectonic forces. *Acta Petrolei Sinica* 13 (1), 1–12.

Wen, Z., Kang, Y. S., Ze, D., Sun, L. Z., Li, G. Z., and Wang, H. Y. (2019). Characteristics and distribution of current *in-situ* stress at shallow-medium-depth in coal-bearing basins in China. *Geological Review* 65 (3), 729–742.

Wu, J., Liu, X.J., Ma, Z.J., and Han, D. 2018. Tectonic genesis of Linxing Block and its influence on oil and gas accumulation. *National Coalbed Methane Symposium*. Beijing: Petroleum Industry Press:47–54.

Yalçin, E., and Durucan, A. 1991. Methane desorption characteristics of Zonguldak coals. *Min. Sci. Technol.* 13 (2), 207–214.

Zhi, D. M., and Xue, L. (2013). *Coalbed methane resources and exploration potential in Junggar Basin*. Bejing: Petroleum Industry Press, 167.